
Adjoint-Based Control of Model and Discretization Errors for Gas and Water Supply Networks

Pia Domschke, Oliver Kolb and Jens Lang

Department of Mathematics, Technische Universität Darmstadt

Dolivostr. 15, D-64293 Darmstadt, Germany

Center of Smart Interfaces, Technische Universität Darmstadt

Petersenstr. 30, D-64287 Darmstadt, Germany

Graduate School Computational Engineering, Technische Universität Darmstadt

Dolivostr. 15, D-64293 Darmstadt, Germany



TECHNISCHE
UNIVERSITÄT
DARMSTADT

Research Group
Numerical Analysis and
Scientific Computing

December 1, 2010

Abstract

We are interested in the simulation and optimization of gas and water transport in networks. Those networks consist of pipes and various other components like compressor/pumping stations and valves. The flow through the pipes can be described by different models based on the Euler equations, including hyperbolic systems of partial differential equations. For the other components, algebraic or ordinary differential equations are used. Depending on the data, different models can be used in different regions of the network. We present a strategy that adaptively applies the models and discretizations, using adjoint-based error estimators to maintain the accuracy of the solution. Finally, we give numerical examples for both types of networks.

1 Introduction

The operation of gas and water supply networks plays an important role in the public utility infrastructure. Both are supposed to work reliably and efficiently as well for economical as ecological reasons. Therefore, the support of gas and water suppliers with software tools is of great common interest. While monitoring systems are already quite advanced, efficient simulation and optimization tools are only available to some extent. Of course, before optimization tasks can be considered, reliable simulation algorithms are essential. In this context, reliability implies robustness as well as trustworthy error estimates.

In the field of simulation and optimization of gas and water supply networks, a lot of research has been done in the last years, for example [5, 8, 9, 10, 12, 13]. Usually, especially for optimization problems, fixed models and also fixed discretizations are considered. Existent software packages like SIMONE [16] allow to use stationary as well as transient models for the simulation of gas networks. However, for the simulation process, one model has to be chosen in advance. SIMONE is also able to solve optimal control problems, but only steady state models are used here. In [8, 5], where nonlinear programming techniques are used to solve optimal control problems for gas and water supply networks, full a priori discretizations in time and space are applied to the underlying equations. Similarly, in [12, 13], where mixed-integer linear programming is proposed for gas network optimization, fixed models and fixed discretizations are used. Moreover, the applied discretizations are typically quite coarse to keep the complexity of the resulting problems treatable.

While the application of coarse discretizations or simplified models is often adequate in many parts of the considered networks to resolve the dynamics in the daily operation of gas and water supply networks, no information about the quality of the computed solutions is provided in all mentioned approaches. In [3, 4], a posteriori estimates for the modeling and discretization errors are introduced for finite element approximations. There, adjoint calculus is applied to measure the influence of both errors separately on a given quantity of interest. Recently, we have published an algorithm to adaptively control model and discretization errors in simulations for gas supply networks [6, 7]. This is considered to be the first step towards an efficient optimization framework with reliable error estimates. Due to various similarities, the applied concept of adjoint-based error estimators on a network can as well be used for water supply networks, which are also considered here.

This chapter is organized as follows. We begin with a description of the underlying model equations of gas and water supply networks in Section 2. Afterwards, we derive error estimators for the model and discretization error with respect to a given quantity of interest (Section 3). In Section 4, we present an algorithm, where these estimators are used to adaptively control the model and discretization errors. Finally, numerical results are presented for a gas and a water supply network in Section 5.

2 Modelling

In this section, we give a brief introduction into the modelling of gas and water supply networks. We begin with some general aspects concerning the models of both types of networks before we describe the particular components of each.

2.1 General Aspects

The flow of gas or water through pipelines is a directed quantity, which can be adequately described in one space dimension. Since we need to give the pipes an orientation, we model gas and water supply networks as a directed graph $\mathcal{G} = (\mathcal{J}, \mathcal{V})$ with arcs \mathcal{J} and vertices \mathcal{V} (nodes, branching points).

Typically, the set of arcs \mathcal{J} mainly consists of pipes $\mathcal{J}_p \subseteq \mathcal{J}$, where we have a hierarchy of models to describe the underlying gas/water dynamics. For the computations, one of these models is chosen for each pipe in each time step. From top to bottom, each model in the hierarchy results from the previous one by making simplifying assumptions. In the case of gas networks, we have a hierarchy of three models, while we consider only two models to describe the flow of water. In both cases, the most complex model consists of a hyperbolic system of partial differential equations (PDEs). Due to the spatial dimension, we define an interval $[x_j^a, x_j^b]$ with $x_j^a < x_j^b$ for each pipe $j \in \mathcal{J}_p$. In the case of gas transport, the considered networks also consist of compressor stations, valves and control valves, while we have pumping stations, valves and tanks in water supply networks. These components are described by algebraic equations or ordinary differential equations. Although there is no continuous spatial dimension for these components, we also use the spatial coordinates x_j^a and x_j^b to describe states at the beginning and end of an arc $j \in \mathcal{J} \setminus \mathcal{J}_p$. Alternatively, we denote ingoing and outgoing states with a subscript.

In addition to the equations on the arcs of the network, it is necessary to specify adequate initial, coupling and boundary conditions, which is not trivial in the case of hyperbolic equations (see for instance [2]). Let $v \in \mathcal{V}$ be an arbitrary node with ingoing arcs δ_v^- and outgoing arcs δ_v^+ . Then, Kirchhoff's first rule states that the sum of currents flowing into that node is equal to the sum of currents flowing out of that node (conservation of mass):

$$\sum_{j \in \delta_v^+} q(x_j^a, t) - \sum_{j \in \delta_v^-} q(x_j^b, t) = q(v, t) \quad \forall t > 0 \quad (1)$$

with an auxiliary variable $q(v, t)$, which can be used to model feed-in or demand (see below). For a unique solution, it does not suffice to only claim (1). A further condition which is commonly used in practice is the equality of pressure at the node $v \in \mathcal{V}$, that is,

$$\begin{aligned} p(x_j^a, t) &= p(v, t) \quad \forall j \in \delta_v^+, \\ p(x_i^b, t) &= p(v, t) \quad \forall i \in \delta_v^-, \end{aligned} \quad (2)$$

with an auxiliary variable $p(v, t)$ for the pressure at the node. In water supply networks, the pressure p is typically replaced by the pressure head h .

In this work, we use equality of pressure (2) together with the conservation of mass (1). Due to the hyperbolic nature of the underlying partial differential equations, there is one degree of freedom for either boundary of each arc. This means, at a node $v \in \mathcal{V}$ with m ingoing and n outgoing arcs, we have $m + n + 2$ degrees of freedom (including $p(v, t)$ and $q(v, t)$) but only $m + n + 1$ equations. Thus, we need one further equation at the node v :

$$e(p(v, t), q(v, t)) = 0.$$

At branching points in the network, we typically have

$$q(v, t) = 0,$$

and at boundary nodes, we use

$$p(v, t) = p_v(t)$$

or

$$q(v, t) = q_v(t)$$

with given profiles $p_v(t)$ or $q_v(t)$. According to (1), $q(v, t) > 0$ corresponds to a feed-in of gas/water into the network and $q(v, t) < 0$ to a demand.

2.2 Gas Supply Networks

In this section, we want to have a closer look on how the flow through gas networks is modelled. As mentioned in Sect. 2.1, the network consists of pipes, compressor stations, valves and control valves.

2.2.1 Pipes

The models describing gas flow in pipelines are based on the *Euler equations*, a hyperbolic system of nonlinear partial differential equations. The system consists of the conservation of mass, momentum and energy together with the equation of state for real gases. The transient flow of gas may be described appropriately by equations in one space dimension, pressure losses due to friction are modelled via a source term. A common simplification, the restriction to isothermal flows, that is, flows with constant temperature, makes the energy equation become redundant. The resulting equations are called *isothermal Euler equations*. If we assume a constant speed of sound and let the pipes be horizontal, the equations result in the *nonlinear model* [2]

$$p_t + \frac{\rho_0 c^2}{A} q_x = 0, \quad (3a)$$

$$q_t + \frac{A}{\rho_0} p_x + \frac{\rho_0 c^2}{A} \left(\frac{q^2}{p} \right)_x = - \frac{\lambda \rho_0 c^2 |q| q}{2dAp}. \quad (3b)$$

Here, q denotes the flow rate under standard conditions (1 atm air pressure, temperature of 0 °C), p the pressure, c the speed of sound, λ the friction coefficient, d the diameter, A the cross-sectional area of the pipe and ρ_0 the density under standard conditions.

Neglecting the nonlinear term in the spatial derivative of the momentum equation (3b) yields the *semilinear model*. This simplification is motivated by the slow velocity of gas in real networks. We get

$$p_t + \frac{\rho_0 c^2}{A} q_x = 0, \quad (4a)$$

$$q_t + \frac{A}{\rho_0} p_x = - \frac{\lambda \rho_0 c^2 |q| q}{2dAp}. \quad (4b)$$

A further simplification leads to a (*quasi*-)stationary model: Setting the time derivatives in (4) to zero results in an ordinary differential equation, which can be solved analytically:

$$q = \text{const.}, \quad (5a)$$

$$p(x) = \sqrt{p(x_0)^2 + \frac{\lambda \rho_0^2 c^2 |q| q}{dA^2} (x_0 - x)}. \quad (5b)$$

Here, $p(x_0)$ denotes the pressure at an arbitrary point $x_0 \in [x_j^a, x_j^b]$. Setting $x_0 = x_j^a$, that is the inbound of the pipe, and $x = x_j^b$, that is the end of the pipe, yields the so-called *algebraic model* [15].

2.2.2 Compressor Stations

A compressor station is a facility that increases the pressure of the gas. Running a compressor is relatively costly, since the compressor station consumes some of the gas, that means,

$$q_{\text{out}} = q_{\text{in}} - F_c(p_{\text{in}}, p_{\text{out}}, q_{\text{in}}). \quad (6)$$

The equation for the fuel consumption of the compressor $c \in \mathcal{J}_c \subseteq \mathcal{J}$ is given by

$$F_c(p_{\text{in}}, p_{\text{out}}, q_{\text{in}}) = d_{F,c} q_{\text{in}} \left(\left(\frac{p_{\text{out}}}{p_{\text{in}}} \right)^{\frac{\gamma-1}{\gamma}} - 1 \right), \quad (7)$$

with $p_{\text{in}} = p(x_c^a, t)$, $p_{\text{out}} = p(x_c^b, t)$, $q_{\text{in}} = q(x_c^a, t)$ and $q_{\text{out}} = q(x_c^b, t)$ [10]. Here, γ is the isentropic coefficient of the gas. The coefficient $d_{F,c}$ is a compressor specific constant. The increase in pressure, performed by the compressor station c , is denoted by

$$\Delta_c p(t) = p_{\text{out}} - p_{\text{in}} \quad (8)$$

and depends on the compressor power

$$P_c(p_{\text{in}}, p_{\text{out}}, q_{\text{in}}) = d_{P,c} q_{\text{in}} \left(\left(\frac{p_{\text{out}}}{p_{\text{in}}} \right)^{\frac{\gamma-1}{\gamma}} - 1 \right), \quad (9)$$

with a compressor specific constant $d_{P,c}$. Either (8) or (9) is typically used as control variable.

2.2.3 Valves

Valves are used to regulate the flow of the gas by opening or closing. In case of an open valve, the equations

$$\begin{aligned} q_{\text{in}} &= q_{\text{out}}, \\ p_{\text{in}} &= p_{\text{out}} \end{aligned}$$

hold. If the valve is closed, then

$$q_{\text{in}} = q_{\text{out}} = 0.$$

2.2.4 Control Valves

Control valves, sometimes also referred to as regulators [8], are valves that reduce the gas pressure by a controlled amount. The behaviour of a control valve is modelled via

$$p_{\text{in}} - p_{\text{out}} \stackrel{!}{=} u$$

with control variable $u = u(t)$. The ingoing and outgoing flow rates are identical:

$$q_{\text{in}} = q_{\text{out}}.$$

2.3 Water Supply Networks

Water supply networks feature similar structures as gas supply networks. Here, the main components are pipes, pumps, valves and tanks.

2.3.1 Pipes

To describe the dynamics inside the pipes of a water supply network, we consider two different models, which can for instance be found in [1]. The most complex model, considering the elastic effects, is given by the so-called *water hammer equations*,

$$\frac{gA}{a^2}h_t + q_x = 0, \quad (10a)$$

$$q_t + gAh_x = -\lambda \frac{q|q|}{2DA}, \quad (10b)$$

a *semilinear* hyperbolic system of partial differential equations, where the piezometric head h and the flow rate q are the space and time-dependent state variables. The gravitational constant is denoted by g , a is the speed of sound in the pipe, A and D are the cross-sectional area and the diameter of the pipe, respectively. The right hand side of (10b) models the influence of friction, where λ is the friction coefficient.

A simplified model for the water dynamics inside the pipes can be derived by neglecting the time derivatives in (10). The resulting (*quasi-*)*stationary* or *algebraic* model reads

$$q_x = 0, \quad (11a)$$

$$h_x = -\lambda \frac{q|q|}{2gDA^2}. \quad (11b)$$

Thus, the flow rate is constant in the pipe,

$$q_{\text{in}} = q_{\text{out}}, \quad (12)$$

and the entire pressure head loss is given by

$$h_{\text{in}} - h_{\text{out}} = \lambda \frac{L}{2gDA^2} q|q|, \quad (13)$$

where L denotes the length of the pipe, and h_{in} and h_{out} the ingoing and outgoing pressure head, respectively.

2.3.2 Pumps

Pumps are installed in water supply networks to generate or maintain a certain pressure. Typically, the relation between the flow rate through a pump and the resulting pressure increase is described by a set of *characteristic curves*. A commonly used form for a single curve (see e.g. [5]) is

$$H(q) = h_{\text{out}} - h_{\text{in}} = \alpha_0 - \alpha_r q^r \quad (14)$$

with

$$q = q_{\text{in}} = q_{\text{out}} \quad (15)$$

and $r \in \mathbb{R}_+$. If multiple curves are given, the parameters α_0 and α_r depend on the current speed ω of the pump.

The running costs of a pump result from the power consumption of its motor. Applying an efficiency curve $\eta_c(q)$ as in [14, pp. 36–37] or [9, p. 46], the costs of each pump $c \in \mathcal{J}_c \subseteq \mathcal{J}$ are proportional to

$$P_c(h_{\text{in}}, h_{\text{out}}, q) = \frac{(h_{\text{out}} - h_{\text{in}})q}{\eta_c(q)}. \quad (16)$$

Again, if multiple curves are given to characterize the pump, the efficiency η additionally depends on the speed of the pump.

2.3.3 Valves

There are various kinds of valves installed in water supply networks to control the flow rate and pressure. Here, we consider gate valves, where the opening can be externally controlled.

With $u \in [0, 1]$ being the control variable for the fraction of the opening, we apply

$$u^2(h_{\text{in}} - h_{\text{out}}) = \zeta q |q|, \quad (17)$$

with the friction loss coefficient ζ and

$$q = q_{\text{in}} = q_{\text{out}}. \quad (18)$$

2.3.4 Tanks

Water tanks are used to store water at certain positions in the network. The ingoing flow at the bottom of a tank is given by

$$q = C \text{sign}(h_{\text{outer}} - h_{\text{inner}}) \sqrt{|h_{\text{outer}} - h_{\text{inner}}|} \quad (19)$$

with the discharge coefficient C . Here, h_{outer} denotes the outer pressure head in front of the inlet of the tank and h_{inner} is the inner pressure head at the bottom of the tank, which is the sum of the elevation of the tank and the current stage:

$$h_{\text{inner}} = \text{elevation} + \text{stage}. \quad (20)$$

Note that formally

$$q = q(x_j^a, t), \quad h_{\text{outer}} = h(x_j^a, t), \quad h_{\text{inner}} = h(x_j^b, t)$$

for each tank $j \in \mathcal{J}$.

The change of the stage and therewith the change of h_{inner} is modelled by an ordinary differential equation:

$$\frac{d}{dt} h_{\text{inner}} = \frac{1}{A} q, \quad (21)$$

where A is the cross-sectional area of the tank.

Additionally to the ingoing flow at the bottom of the tank (given by (19)), there can be further inflow or outflow openings, e.g. for refilling the tank or overflow. Concerning the model equations, those terms can be simply added to q in (21) and formally refer to $q(x_j^b, t)$.

3 Error Estimators

For given initial and boundary conditions as well as control states for the controllable elements, the described model equations on the whole network can be solved applying appropriate discretization schemes. For the discretization of the (hyperbolic) PDEs in the pipes, we apply an implicit box scheme [11], which perfectly matches the properties of the underlying equations. The time steps of this scheme are also used to discretize the ordinary differential equations as occurring in the model of water tanks. So far, one step methods are implemented for this purpose and delivered satisfying results.

Now, we are searching for a compromise between the accuracy of the numerical solution and the computational costs. We want to use the more complex models in the pipes only when necessary and to refine the discretizations only where needed. Using the solution of adjoint equations as done in [3, 4, 2, 6, 7], one may deduce model and discretization error estimators to measure the influence of the model and the discretization on a user-defined target functional M . With u being the exact solution of

the (most complex) model equations and u^h being the approximate (numerical) solution for some choice of models, the error in the target functional can be approximated by

$$M(u) - M(u^h) \approx \eta_m + \eta_h, \quad (22)$$

where η_m estimates the model error and η_h the error resulting from the discretization. Concerning the underlying adjoint equations, these error estimators are currently implemented in a first-discretize manner, which will be briefly described in the following. A more detailed description with some hints on the implementation can be found in [7].

Let t_j ($j = 0, \dots, N$) be the times of the discretization. Accordingly, we split up the solution of the discretized model equations

$$(u^h)^T = ((u_0^h)^T, \dots, (u_N^h)^T).$$

Starting with the given initial state u_0^h , we have to solve a system of the form

$$F_j(\underbrace{u_{j-1}^h}_{u_{\text{old}}}, \underbrace{u_j^h}_{u_{\text{new}}}) = 0 \quad (23)$$

in each time step. In the adaptive algorithm described in the next section, we will partition the entire simulation horizon in several blocks. Accordingly, we define

$$(U_k^h)^T = ((u_{j(k-1)+1}^h)^T, \dots, (u_{j(k)}^h)^T)$$

for $k = 1, \dots, N_B$, where $j(k)$ is given via

$$t_{j(k)} = T_k$$

for $k = 0, \dots, N_B$. For later use, we also define

$$(E_k)^T = ((F_{j(k-1)+1})^T, \dots, (F_{j(k)})^T), \quad (24)$$

which summarizes the state-defining equations of the block $[T_{k-1}, T_k]$.

Now, we can estimate the model error of the k th block with respect to the functional M via

$$\eta_{m,k} = \frac{\partial}{\partial U_k} M(u^h) \Delta U_k^h, \quad (25)$$

where

$$\Delta U_k^h = U_k - U_k^h.$$

Here, U_k formally denotes a reference solution in the k th block which solves a different system of equations \tilde{E}_k based on more complex or simpler models. Thus, the difference ΔU_k^h results from the differences in the models and can be estimated by

$$\Delta U_k^h \approx -\left(\frac{\partial}{\partial U_k} \tilde{E}_k(u^h)\right)^{-1} \Delta \tilde{E}_k \quad (26)$$

with

$$\Delta \tilde{E}_k = \tilde{E}_k(U_k^h) - \underbrace{\tilde{E}_k(U_k)}_{=0} = \tilde{E}_k(U_k^h). \quad (27)$$

Inserting (26) and (27) in (25) finally gives

$$\eta_{m,k} = -\frac{\partial}{\partial U_k} M(u^h) \left(\frac{\partial}{\partial U_k} \tilde{E}_k(u^h) \right)^{-1} \tilde{E}_k(U_k^h) = -\xi_k^T \tilde{E}_k(U_k^h)$$

with ξ_k being the solution of the *adjoint equation*

$$\left(\frac{\partial}{\partial U_k} \tilde{E}_k(u^h) \right)^T \xi_k = \left(\frac{\partial}{\partial U_k} M(u^h) \right)^T. \quad (28)$$

Instead of $\frac{\partial}{\partial U_k} \tilde{E}_k(u^h)$ one may also apply $\frac{\partial}{\partial U_k} E_k(u^h)$ in (28) to get an error estimation. This way, it suffices to solve one system of adjoint equations (per block) for the estimators with respect to higher and lower models and also with respect to the discretization. Moreover, note that (28) can be solved very efficiently due to the special structure of \tilde{E}_k and E_k (see [7]).

Regarding the derivation of the model error estimator $\eta_{m,k}$ above, one may observe that an error estimator for discretization errors can be deduced in exactly the same way. Here, the reference solution U_k resulting from solving a modified system of equations \tilde{E}_k must refer to another discretization. In our implementation, the residual $\tilde{E}_k(U_k^h)$ is estimated by comparing the single terms in the applied discretization scheme with reconstruction formulas of higher order. This way, separate error estimators for the temporal and the spatial error (for each element in each block) can be evaluated:

$$\eta_{h,k} = \eta_{x,k} + \eta_{t,k}, \quad (29)$$

where $\eta_{x,k}$ denotes the estimator for the spatial error and $\eta_{t,k}$ for the temporal error in the k th block [6, 7].

4 Adaptive Error Control

In the last section, we have developed error estimators for model and discretization errors. With these estimators, we can now control the computational errors inside the network. Since in practice the dynamic behaviour in the network varies, we want to control the relative error resulting from the choice of the models and the discretization in blocks of several time steps. Thus, we divide the time interval $[0, T]$ into blocks of equal size $[T_{k-1}, T_k]$, $k = 1, \dots, N_B$. Regarding one subinterval $[T_{k-1}, T_k]$, we can compute the forward as well as the backward/adjoint solution and evaluate the error estimators locally, which yields

$$M_k(u) - M_k(u^h) \approx \eta_{m,k} + \eta_{t,k} + \eta_{x,k}.$$

Given a tolerance TOL for the relative error, we can approximate the exact error by the estimators, giving

$$\frac{|M_k(u) - M_k(u^h)|}{|M_k(u)|} \approx \frac{|\eta_{m,k} + \eta_{t,k} + \eta_{x,k}|}{|M_k(u^h)|} \stackrel{!}{\leq} \text{TOL}. \quad (30)$$

We first examine the discretization error to ensure the discretization to be adequate. Then we consider the model error.

Check Discretization Error. First, the discretization is checked. Given the tolerance TOL as above, we ensure the discretization error to be small enough by decreasing TOL by a user-defined factor $0 < \kappa < 1$ giving $\text{TOL}_h := \kappa \cdot \text{TOL}$. We demand the discretization error estimator to satisfy

$$|\eta_{t,k} + \eta_{x,k}| \leq \text{TOL}_h \cdot |M_k(u^h)|.$$

If the error estimator exceeds the given upper bound, the temporal and spatial discretization errors are treated individually, that is,

$$|\eta_{t,k}| \leq \frac{1}{2} \text{TOL}_h \cdot |M_k(u^h)| \quad \text{and} \quad |\eta_{x,k}| \leq \frac{1}{2} \text{TOL}_h \cdot |M_k(u^h)|.$$

Check Temporal Discretization Error. If the temporal error estimator exceeds the given tolerance, the time step size is marked for refinement. After checking the spatial discretization error, the time interval $[T_{k-1}, T_k]$ has to be computed again. If, in contrast, the error estimator $|\eta_{t,k}|$ is much smaller than the upper bound, the time step size is marked for coarsening. If the current time interval has to be recomputed due to spatial or model errors, the temporal coarsening is not applied.

Check Spatial Discretization Error. Now, the spatial discretization error is estimated locally for each pipe,

$$\eta_{x,k} = \sum_{j \in \mathcal{J}_p} \eta_{x,k,j}.$$

Thus, we want to satisfy

$$\left| \sum_{j \in \mathcal{J}_p} \eta_{x,k,j} \right| \leq \frac{1}{2} \text{TOL}_h \cdot |M_k(u^h)|.$$

For this inequality to hold, it suffices to claim

$$\sum_{j \in \mathcal{J}_p} |\eta_{x,k,j}| \leq \frac{1}{2} \text{TOL}_h \cdot |M_k(u^h)|.$$

In order to get an upper bound for each pipe itself, we uniformly distribute the target functional, i.e., we divide it by the number of pipes $|\mathcal{J}_p|$, giving

$$|\eta_{x,k,j}| \leq \frac{1}{2} \text{TOL}_h \cdot \frac{|M_k(u^h)|}{|\mathcal{J}_p|} \quad \forall j \in \mathcal{J}_p.$$

If $|\eta_{x,k,j}|$ exceeds the given tolerance, the pipe is marked for refinement. If, instead, the error estimator is much smaller than the right hand side, the pipe is marked for coarsening. The time interval $[T_{k-1}, T_k]$ is computed again with a finer discretization where needed.

Check Total Error. If the discretization error is small enough, the total error estimator $\eta_{m,k} + \eta_{t,k} + \eta_{x,k}$ is evaluated. If

$$|\eta_{m,k} + \eta_{t,k} + \eta_{x,k}| > \text{TOL} \cdot |M_k(u^h)|,$$

that is, the total error does not fit the desired tolerance while the discretization error did, the model error is checked.

Check Model Error. If the discretization error is small enough, but the total error is not, the model errors of all pipes are checked. Again, we uniformly distribute the target functional over all pipes. If the error estimator exceeds the given tolerance, that is,

$$|\eta_{m,k,j}| > \text{TOL}_m \cdot \frac{|M_k(u^h)|}{|\mathcal{J}_p|},$$

with $\text{TOL}_m := (1 - \kappa) \cdot \text{TOL}$, the pipe is supposed to use the model above subject to the hierarchy. The time interval $[T_{k-1}, T_k]$ is computed again with the adjusted models.

Coarsen Temporal and/or Spatial Discretization and Switch Down Models. If the total error fits the desired tolerance, the time interval $[T_{k-1}, T_k]$ is accepted and k is increased. If the time step size or any pipes were marked for coarsening, the coarsening is applied. Then, the estimators with respect to the lower models are computed. If the error estimator is much less than the given tolerance, that is,

$$|\eta_{m,k,j}| \leq s \cdot \text{TOL}_m \cdot \frac{|M_k(u^h)|}{|\mathcal{J}_p|},$$

with a “shift down factor” $s \ll 1$ (e.g. 10^{-1} or 10^{-2}), the pipe can use the lower model for the next calculations and we go on to the next interval.

5 Numerical Examples

In this section, we give numerical results for a medium sized real life gas network and a water supply network. All presented computations were done on an AMD Athlon™ 64 X2 Dual Core 6000+.

5.1 Gas Supply Network

We begin with the gas supply network, which is shown in Fig. 1. The considered network consists of twelve pipes (P01 – P12, with lengths between 30km and 100km), two sources (S01 – S02), four consumers (C01 – C04), three compressor stations (Comp01 - Comp03) and one control valve (CV01).

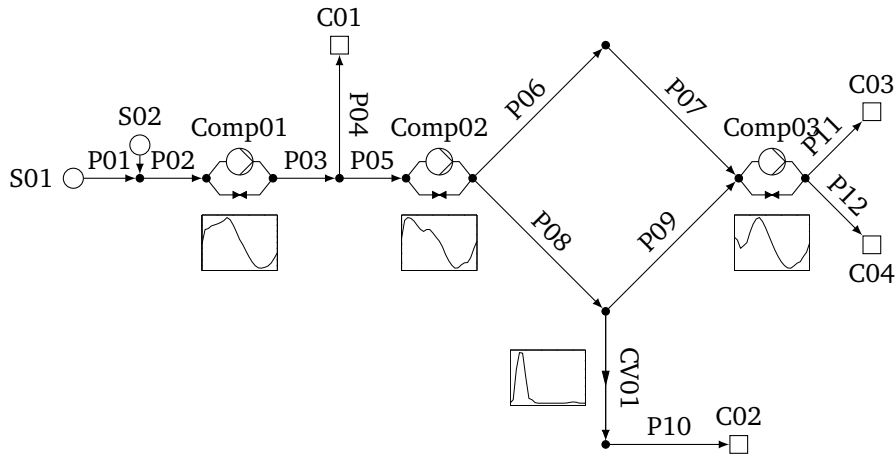


Figure 1: Gas supply network with compressor stations and control valve

The simulation starts with stationary initial data. The boundary conditions and the control for the compressor stations and the control valve are time-dependent. Plots of the control functions are given in Fig. 1. The target functional is given by the total fuel gas consumption of the compressors, i.e.

$$M(u) = \sum_{c \in \mathcal{J}_c} \int_0^T F_c(t) dt.$$

The simulation time is 86,400 seconds (24 hours) with an initial time step size $\Delta t = 3,600$ seconds. The subintervals are 7,200 seconds (2 hours) each. The initial spatial step size is $\Delta x = 10,000$ m. The factor κ is set to 10^{-1} and the shift down factor $s = 10^{-1}$. The tolerance TOL is set to values between 10^{-1} and 10^{-4} .

Table 1 shows the maximal relative error in the target functional

$$\text{rel.err.} = \max_k \frac{|M_k(u) - M_k(u^h)|}{|M_k(u)|}, \quad (31)$$

the total target functional, the maximal and the minimal time and spatial step size used subject to the tolerance TOL and the running time. As an approximation of the exact solution we computed a solution with the nonlinear model and a finer discretization than used in the adaptive algorithm, which is shown in the last row.

Table 1: Results using different values for TOL

TOL	rel.err.	$M(u^h)$	max/min Δt	max/min Δx	time [s]
1e-01	1.690905e-01	5.0480603810e+01	3600/900	33,333.3/10,000	2.7e-01
1e-02	1.756343e-02	4.8408860265e+01	900/450	33,333.3/10,000	1.0e+00
1e-03	1.288994e-03	4.8487439184e+01	225/28.125	16666.7/1,250	3.5e+01
1e-04	4.010694e-05	4.8486374440e+01	14.0625/1.7578	16666.7/312.5	1.0e+03
reference solution		4.8485402013e+01	1	312.5	4.2e+03

Generally, we observe that the maximal relative error decreases with the tolerance TOL. We can also see that the error estimators do not provide a sharp upper bound for the error.

Besides the discretization, it is also interesting how the model switching part works depending on TOL. Table 2 shows how often which model is used during the simulation. The trend is the same as for the discretization. For smaller tolerances, the share of the more complex models is higher.

Table 2: Models used during simulation for different values of TOL

TOL	ALG	LIN	NL
1e-01	100%	0%	0%
1e-02	46.7%	53.3%	0%
1e-03	13.7%	85%	1.3%
1e-04	2.5%	73.7%	23.7%

5.2 Water Supply Network

As a second example, we consider the water supply network shown in Fig. 2. The network consists of sixteen pipes (P01 – P16, with lengths between 500m and 20km), two suppliers (S01 – S02), six consumers (C01 – C06), three pumps (Pump01 - Pump03), four tanks (T01 – T04) and two valves (V01 – V02).

The simulation starts with approximately stationary data. The boundary conditions as well as the control for the pumps and the valves are time-dependent. As above, plots of the control functions are given in Fig. 2. The target functional is given by the total energy consumption of the pumps, which is proportional to

$$M(u) = \sum_{c \in \mathcal{J}_c} \int_0^T P_c(t) dt.$$

The simulation time is 86,400 seconds (24 hours) with an initial time step size $\Delta t = 3,600$ seconds. The subintervals are 7,200 seconds (2 hours) each. The initial spatial step size has been chosen as coarse as possible such that the applied (spatial) error estimators can be evaluated, that is exactly four grid points

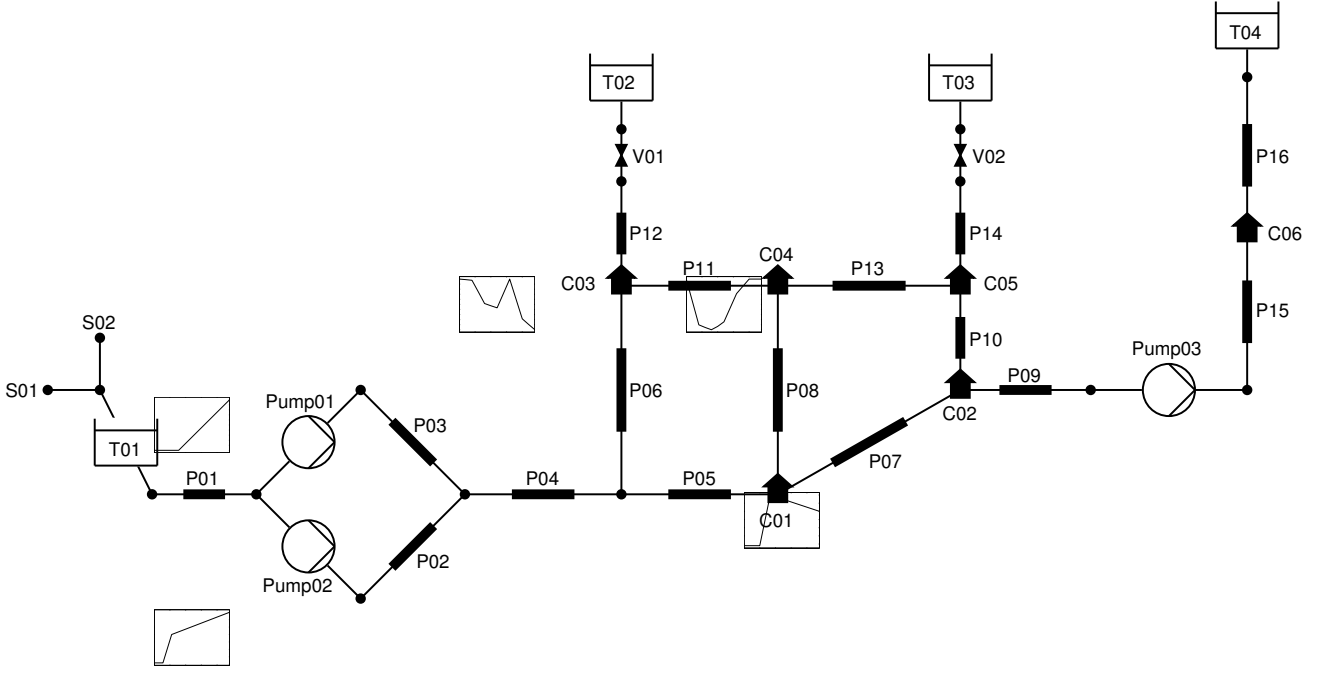


Figure 2: Water supply network with pumps, valves and tanks

per pipe. Similar to above, the factor κ is set to 10^{-1} and the shift down factor $s = 10^{-1}$. The tolerance TOL is set to values between 10^{-1} and 10^{-4} .

Table 3 shows the maximal relative error in the target functional according to (31), the total target functional, the maximal and the minimal time and spatial step size used subject to the tolerance TOL and the running time. As an approximation of the exact solution we computed a solution with the time-dependent model and a finer discretization than used in the adaptive algorithm, which is shown in the last row.

Table 3: Results using different values for TOL

TOL	rel.err.	$M(u^h)$	max/min Δt	max/min Δx	time [s]
1e-01	1.228465e-02	8.3184539798e+01	3600/900	6666.7/166.7	5.4e-01
1e-02	1.491658e-03	8.3079443781e+01	900/225	6666.7/166.7	1.9e+00
1e-03	9.460297e-04	8.3014423132e+01	112.5/28.125	6666.7/166.7	9.7e+00
1e-04	7.546011e-05	8.3037462607e+01	14.0625/3.5156	6666.7/166.7	1.6e+02
reference solution		8.3038197026e+01	2	100	1.5e+03

As above, we observe that the maximal relative error in each block decreases with TOL. Moreover, the error tolerance is satisfied here. Obviously, the time discretization plays the crucial role in this example. The initial spatial discretization is not refined. Additionally, the difference between the two models only becomes important for the smallest tolerance, which can be seen from Tab. 4.

Table 4: Models used during simulation for different values of TOL

TOL	ALG	LIN
1e-01	100%	0%
1e-02	100%	0%
1e-03	100%	0%
1e-04	42.2%	57.8%

6 Conclusion and Outlook

We have addressed the simulation task for gas and water supply networks based on a hierarchy of models for the gas/water dynamics in the pipes. Further network components modelled by algebraic and ordinary differential equations have been considered. Using adjoint equations, we introduced error estimators to measure the influence of the discretization in time and space and the applied models with respect to a given target functional. With these estimators, we developed an algorithm to adaptively control the different errors within a given tolerance.

We gave examples for both types of networks to show the applicability of the algorithm. In both cases, it could be seen that the actual errors decreased with the prescribed tolerance. By construction, the error estimators do not provide an upper bound but are a first order approximation of the true error. For the considered water supply network, all error bounds were maintained. For the gas network, the actual errors were slightly larger than the given tolerance.

The results achieved so far (also in [6, 7]) make us confident that the presented techniques can build a reliable basis to solve optimal control problems for gas and water supply networks. In particular, the sensitivity information computed for the evaluation of the error estimators can be used to compute gradient information for derivative-based optimization. Regarding optimization problems, we will have to consider multiple quantities of interest. These are the objective functional of the given task and all constraints, which are supposed to be evaluated within given tolerances as well.

Another part of our future work is the extension of the presented approach to further applications. The principle of adjoint-based control of model and discretization errors does not stick to gas and water supply networks. Basically, any transport process on networks can be considered. Here, one application we have in mind is traffic flow on networks.

References

- [1] José Abreu, Enrique Cabrera, Joaquín Izquierdo, and Jorge García-Serra. Flow modeling in pressurized systems revisited. *Journal of Hydraulic Engineering*, 125(11):1154–1169, 1999.
- [2] Pia Bales, Oliver Kolb, and Jens Lang. Hierarchical modelling and model adaptivity for gas flow on networks. In *Computational Science - ICCS 2009*, volume 5544 of *Lecture Notes in Computer Science*, pages 337–346. Springer Berlin / Heidelberg, 2009.
- [3] Roland Becker and Rolf Rannacher. An optimal control approach to a posteriori error estimation in finite element methods. *Acta numerica*, 10:1–102, 2001.
- [4] Malte Braack and Alexandre Ern. A posteriori control of modeling errors and discretization errors. *SIAM Journal of Multiscale Modeling and Simulation*, 1(2):221–238, 2003.
- [5] Jens Burgschweiger, Bernd Gnädig, and Marc C. Steinbach. Optimization models for operative planning in drinking water networks. *Optimization and Engineering*, 10(1):43–73, March 2009.
- [6] Pia Domschke, Oliver Kolb, and Jens Lang. An adaptive model switching and discretization algorithm for gas flow on networks. *Procedia Computer Science*, 1(1):1325 – 1334, 2010. ICCS 2010.
- [7] Pia Domschke, Oliver Kolb, and Jens Lang. Adjoint-based control of model and discretisation errors for gas flow in networks. *Int. J. Mathematical Modelling and Numerical Optimisation*, X(X):XXX–XXX, 201X. Accepted for publication.
- [8] Klaus Ehrhardt and Marc Steinbach. Nonlinear optimization in gas networks. ZIB-Report 03-46, December 2003.
- [9] Christian Hähnlein. *Numerische Modellierung zur Betriebsoptimierung von Wasserverteilnetzen*. PhD thesis, TU Darmstadt, 2008.

-
- [10] Michael Herty. Modeling, simulation and optimization of gas networks with compressors. *Networks and Heterogeneous Media*, 2(1):81–97, 2007.
- [11] Oliver Kolb, Jens Lang, and Pia Bales. An implicit box scheme for subsonic compressible flow with dissipative source term. *Numerical Algorithms*, 53(2):293–307, 2010.
- [12] Alexander Martin, Markus Möller, and Susanne Moritz. Mixed integer models for the stationary case of gas network optimization. *Mathematical Programming*, 105:563–582, 2006.
- [13] Susanne Moritz. *A Mixed Integer Approach for the Transient Case of Gas Network Optimization*. PhD thesis, TU Darmstadt, 2006.
- [14] Lewis A. Rossman. *EPANET 2 users manual*. U.S. Environmental Protection Agency, Cincinnati, OH, 2000.
- [15] Erwin Sekirnjak. *Transiente Technische Optimierung (TTO-Prototyp)*. Technical report, PSI AG, November 2000.
- [16] SIMONE Research Group. <http://www.simone.eu>.